Jurnal Teknologi

Full Paper

FLAME PROPAGATION AND BURNING RATES OF METHANE-AIR MIXTURES USING SCHLIEREN PHOTOGRAPHY

Mohd Suardi Suhaimi[a*], Aminuddin Saat[b], Mazlan A. Wahid[b], Mohsin Mohd Sies[b]

[a]Process Systems Engineering Center (PROSPECT), Department of Chemical Engineering, Faculty of Chemical Engineering, Universiti Teknologi Malaysia, 81310 UTM Johor Bahru, Johor, Malaysia
[b]High Speed Reacting Flow Laboratory (HiREF), Department of Thermofluids, Faculty of Mechanical Engineering, Universiti Teknologi Malaysia, 81310 UTM Johor Bahru, Johor, Malaysia

Article history
Received
29 April 2016
Received in revised form
15 May 2016
Accepted
22 May 2016

*Corresponding author
msuardi2@live.utm.my

Abstract

Different methodology have been shown to produce different results for Markstein length and laminar burning velocity of methane-air mixture. This study attempts to determine the aforesaid parameters using the newly developed closed vessel combustion chamber with Schlieren photography. Markstein length and burning rate of methane-air mixture was determined under the initial pressure of 1 atm, temperature range of 298-302K and equivalence ratio range of 0.7-1.3. Experiments were performed in a centrally ignited 29.16L cylindrical constant volume combustion chamber. Ignition energy was set at 25mJ for each experiment. The images of spherically expanding flame were recorded using Schlieren photography technique at a speed of 2000 frame per second. Analysis of the flame area yield flame radii from which the flame speed and stretch rate could be obtained. These parameters would allow the determination of Markstein length and burning rate of the flame. Results show that Markstein length magnitude increases proportionally with equivalence ratio with a magnitude ranging from 0.125cm to 0.245cm. Maximum burning rate occurs at equivalence ratio of 1.1 with a magnitude of 0.366 m/s. Flame of each equivalence ratio also exhibits fluctuation arising from acoustic disturbance. This disturbance becomes more apparent at higher equivalence ratio.

Keywords: Methane-air, Markstein length, burning rate, Schlieren, closed vessel

1.0 INTRODUCTION

The determination of combustion characteristics such as the Markstein length and laminar burning velocity is of primary importance as it describes both the laminar and turbulent premixed combustion. Detailed knowledge from accurate measurement of laminar premixed flames will provide valuable insight on propagation rates, heat release, flammability limits, quenching and emission characteristics. Another useful insight from laminar premixed flame is that it could serve as a preliminary data in understanding a much more complex combustion such as turbulent non-premixed combustion and also combustion process in practical combustor such as internal combustion engine where the initial stage of combustion involves laminar premixed combustion.

Several methods have been used to determine this parameter such as flat flame [1, 2], counterflow flame [3, 4] and spherically expanding flame [5-8]. These experiments also enable the study of another parameter which is the stretch that acts on the flame front. This parameter is a combination of curvature and strain rate and is described by Markstein length [9].

For spherically expanding flame, the stretch can be obtained analytically from flame speed and radius. The unstretched flame speed on the other hand could be obtained from linear extrapolation of the flame speed and stretch curve [10]. However it is

sensitive to the data obtained from experiment. Earlier work by Taylor [5] involved the differentiation of the spherically expanding flame radius to obtain flame speed, stretch, Markstein length and burning rate. Tahtouh *et al.* [9] compared three different analysis methods namely the polynomial fitting, raw radius differentiation and a new method that involves resolution of Clavin's equation to determine the aforesaid parameters. They reported that each method yield different results.

The objective of this study is to determine the burning rate and Markstein length of methane-air mixture using images from Schlieren photography. Methane is one of the abundant gaseous fuel in nature that also exist in nature as the flammable part of biogas [11]. Schlieren photography is a photography technique that makes use of the density gradient in the vicinity of the object of interest. This is particularly useful in combustion as it generates a region with defined density gradient arising from generated heat. Though the method is not novel, obtaining improved images could improve results from literature. Schlieren photography also permits the exclusion of experiments that produce cellular flame for the purpose of determining flame speed, Markstein length and burning rates [11]. This exclusion is important as the incidence of cellularity will render the smooth flame front assumption void. Comparison with data from literature may also serve as a calibration to the rig setup used in this study.

The laminar flame speed can be obtained from Schlieren photographs as described in [12]. In deriving a relationship for spherically propagating flame, two distinct physical phenomena of stretch should be considered. The first is the tangential strain rate (a_{tt}) on the flame surface while the second is the curved flame propagation. The curved flame propagation could in turn be characterized by arithmetic mean of local curvature (h) and local propagation velocity relative to reactant fluid (S_b). S_b can also be viewed as the propagation of the curved flame relative to its origin. Flame stretch could be expressed in terms of these physical phenomena as:

$$\alpha = a_{tt} + 2S_b h \quad (1)$$

For the case of spherical flame, the flame speed and flame stretch could be expressed as;

$$S_n = \left(\frac{\rho_b}{\rho_u}\right)\frac{dr}{dt} \quad (2)$$

$$\alpha = \left(\frac{2}{r}\right)\frac{dr}{dt} \quad (3)$$

$$\alpha = \left(\frac{2}{r}\right)S_n \quad (4)$$

The term $\left(\frac{\rho_b}{\rho_u}\right)$ represents the density ratio of the burned and unburned gas and computed under the assumption of adiabatic constant pressure combustion. Including the effect of stretch on flame speed yields:

$$S_s - S_n = L_b\alpha \quad (5)$$

Where S_s is the unstretched flame speed and L_b is the proportionality constant called Markstein length. Markstein length represents the extent of stretch rate (α) effect on stretched flame speed S_n and could be obtained as the slope of flame speed against stretch plot. Such plot also gives the unstretched flame speed by extrapolating the plot to a point of zero stretch.

The unstretched flame speed also enables the determination of burning rate, u_L, by the relation:

$$u_L = S_s\frac{\rho_b}{\rho_u} \quad (6)$$

Burning rate, or sometimes referred to as burning velocity could be perceived as the velocity of the cold reactants moving into the reaction zone and normal to the reaction zone plane [10]

2.0 METHODOLOGY

Figure 1 shows the overall experimental setup consisting of a cylindrical constant volume combustion chamber with a volume of 29.3 litre equipped with two 190mm quartz windows, ignition system, Phantom 7.1 highspeed camera, collimating and decollimating lens and an LED light source. Ignition was initiated with Labview 7.1 software that also serves as a data logger recording pressure rise during combustion.

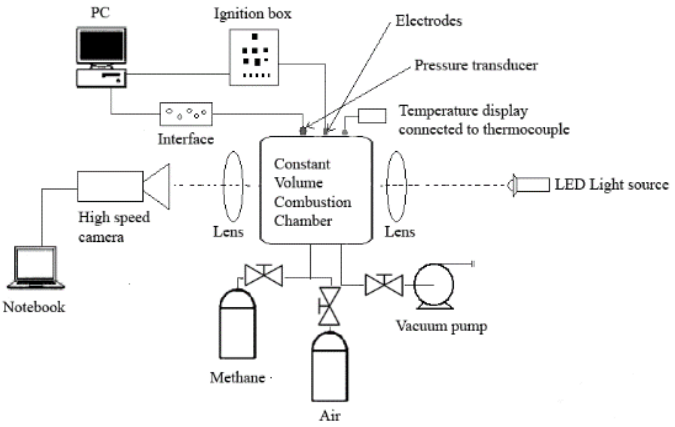

Figure 1 Experimental setup

The cylindrical combustor used in this study is equipped with a pair of opposing spark electrodes to provide ignition at the center of the combustor. After a vacuum was created in the combustion chamber by a vacuum pump, the chamber was filled with methane and dry air using partial pressure filling technique which correspond to the desired equivalence ratio. The initial pressure for each experiment was set at atmospheric pressure, while the initial temperature was in the range of 298 to 302K. Ignition was controlled using a desktop computer with a LabView 7.1 software connected to the ignition box after the capacitor was charged. The 190 mm

windows provide wide optical access and currently limited by the lens used. A pair of collimating and decollimating lens with 150 mm diameter was used. Both lens have a focal length of 700 mm. The developing flame videos were recorded at 2000 frames per second using the phantom high speed camera. A 1.5W LED lamp was used as a light source to illuminate the combustor internal section.

The recorded cine videos were then converted to Schlieren image files for further analysis using image processing software. Adobe Photoshop image editing software was used to convert to the images of the spherical flames to binary images. These binary images were then analyzed using a Matlab script file to obtain flame area and later the radius. The obtained radii were then tabulated in a spreadsheet file where the flame speed was obtained by differentiating with respect to time a first order fit of five points.

3.0 RESULTS AND DISCUSSION

The observation of spherical flame propagation at different equivalence ratio is shown in Figure 2. The methane-air mixtures were centrally ignited by a pair of steel spark electrodes (as indicated by a tilted thick black line in each image) connected to the ignition box, as shown previously in Figure 1. The circular boundary represents the size of the optical access windows. Pre-ignition conditions for each of the experiments were started at atmospheric conditions. In general, all flames show a smooth flame surface and stable development throughout the propagation. As indicated by the size ofspherical flame, the stoichiometric flame developed at a much faster rate compared to other flames at equivalence ratio of 0.8 and 1.3. This corresponds well with the characteristics of burning rates where the burning velocity tends to be higher at equivalence ratio slightly greater than stoichiometric value [13].

From the Schlieren images, the flame radius of each images is calculated and plotted as a function of time after ignition. Figure 3 shows the flame radius of methane-air for two experiments at similar equivalence ratio of 0.8. The flame speed is then calculated from the flame radius as indicated in Figure 4.

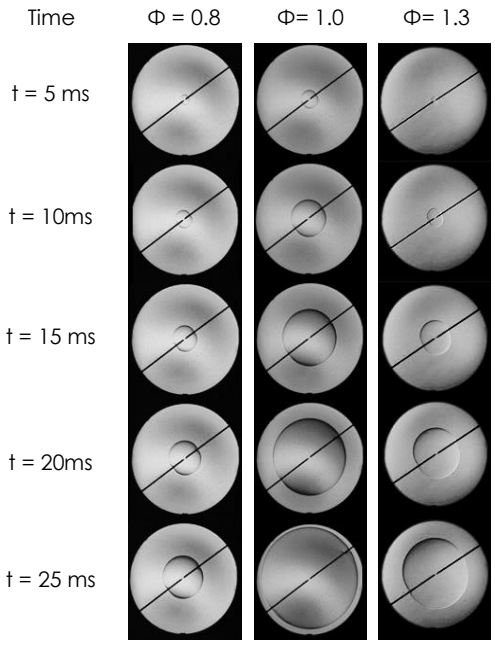

Figure 2 Development of spherical flame of methane-air mixture atdifferent time after ignition for equivalence ratio of 0.8, 1.0 and 1.3

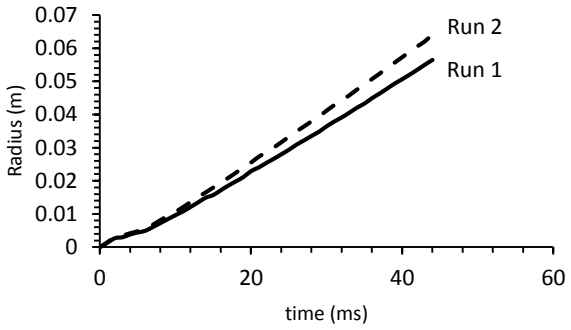

Figure 3 Spherical flame radius changeof methane-air mixture atdifferent time after ignition for equivalence ratio of 0.8

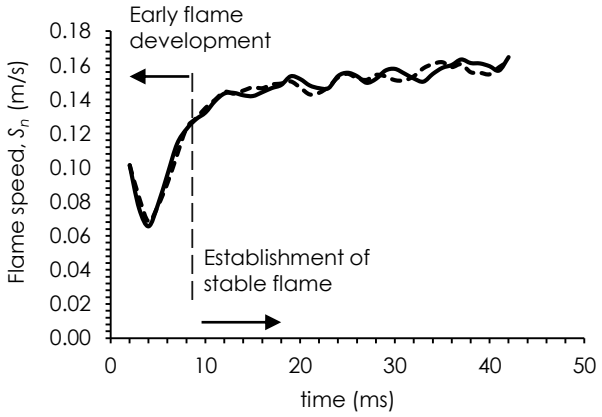

Figure 4 Variation of flame speed of methane-air mixture with time at equivalence ratio of 0.8

Figure 4 shows the comparison of flame speed as a function of time of similar experiment at equivalence ratio of 0.8. The plot depicts a typical flame speed progress over time with a sharp decrease from the point of ignition to a certain time where it reaches a minimum pivotal point. This could be attributed to the radicals from the spark that rapidly dissipates until it reaches the minimum point [6]. The spark also creates shockwave that propagates outward, followed by a slower thermal wave. The thermal wave front usually has high initial speed that rapidly decreases over a short period of time [14]. From the minimum point, flame speed start to increase again until it stabilizes with time as the combustion progresses. Within this region normal chemistry predominates combustion as the radicals from the spark diminishes. Flame establishment can be estimated by the linear relation of flame speed against stretch rate which will be discussed later.

As shown in Figure 4, both experiments also show similar trend with a slight variation suggesting good data reproducibility. The percentage offlame speed fluctuation after 15 ms onwards is around 6.3% which is considerably low. The noticeable fluctuation at 19 ms onwards could be linked to acoustic disturbances as observed by Gillespie *et al.* [10]. The flame-acoustic disturbances are caused by an interaction between heat release and acoustic waves [15]. Curved flames (including spherical flame) are more susceptible to acoustic disturbances, where the propagating flame front is stretched and curved by acoustic waves [16]. This disturbance could also be influenced by combustor geometry [17]. However, the effect of oscillation on flame speed is beyond the scope of this study.

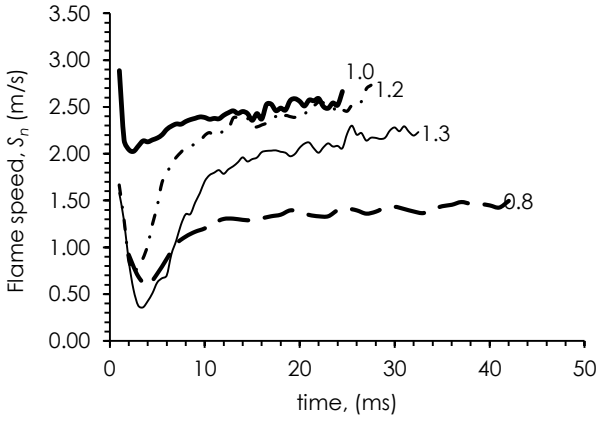

Figure 5 Variation of flame speed of methane-air mixture with time at various equivalence ratios of 0.8, 1.0, 1.2 and 1.3

Figure 5 shows the comparison of flame speed obtained from different equivalence ratio with respect to time. The trend of the flame speed development displays similar trend with a sudden decrease to a minimum point before it increase again to reach an approximately stable speed with noticeable fluctuation. It is interesting to note that, fluctuation commenced after around 15 ms for each experiment. The percentages of fluctuation are 11.6%, 17.8% and 19.0 % for stoichiometric, 1.2 and 1.3 experiments. Apparently, fluctuation is more pronounced at higher equivalence ratio. This might suggest acoustic disturbance, as discussed earlier, is more prevalent at richer side.

In terms of trend, the initial flame speed and the point at which the minimum flame speed occurs is different from each run. This point is highest for flame under stoichiometric condition followed by the flame of 1.2, 0.8 and 1.3. In the early stage of flame propagation, the flame is overcoming the quenching tendency due to high stretch rate arising from curvature effect [18]. Also, the flame speed of 0.8 progressed slower compared other experiments. This is followed by 1.3, 1.2 and lastly 1.0. This indicates the relative speed of the flame under different equivalence ratio. Flames that are either on the leaner or the richer side usually propagates slower than flame under stoichiometric condition. This is due to the disparity in thermal and mass diffusivity magnitude that would affect mass and heat transfer hence the flame propagation; whereas under stoichiometric condition, the magnitude of both thermal and mass diffusivity are equal [19]. The graph also reveals the time at which the flame stabilizes after ignition. The flames of each run took approximately 10 ms to reach an approximately stable flame.

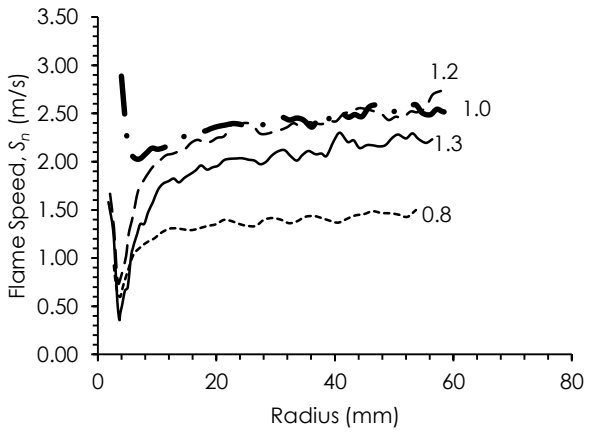

Figure 6 Variation of flame speed of methane-air mixture with radius at various equivalence ratio of 0.8, 1.0, 1.2 and 1.3

Figure 6 shows the plot of flame speed versus radius of methane-air mixture for experiments of 0.8, 1.2 and 1.3 equivalence ratios. The plot shows a periodically scattered data with a trend similar to flame speed variation with time. Fluctuation however is less pronounced in each experiment. At approximately 2 mm radius, the flame reaches its minimum value after ignition. The radius is about 1 mm larger for stoichiometric experiment. From this minimum point

onwards, the flame development is due to normal chemistry. Data with radii less than 10mm should be discarded for burning rate calculation, as within this range the flame is significantly influenced by the radicals and shockwave from the spark [18].

Figure 7 shows the variation of methane-air mixture flame speed with stretch. With the exception of stoichiometric experiment, the variation of flame speed for three other experiments i.e. for equivalence ratio of 0.8, 1.2 and 1.3 shares some similarities especially the characteristics twist during the early stage of flame propagation. This could be attributed to the effect of ignition energy and also to different stretch rate at the early stage of flame development [18]. Apparently stretch rate becomes more obvious under lean and rich region. Extrapolating flame speed to a point of zero stretch rates in Figure 7 yields unstretched flame speed S_s while the slope gives the Markstein length L_b. However, prior to extrapolation, some data especially those represent the early stage of combustion should be excluded as these data are generally affected by ignition spark and could lead to over or underestimation of unstretched flame speed.

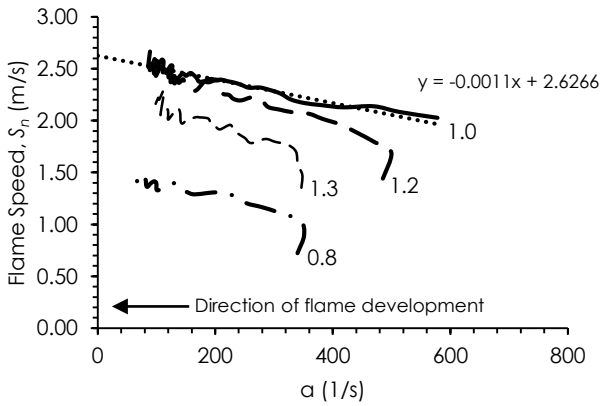

Figure 7 Variation of flame speed of methane-air mixture with stretch rate at various equivalence ratio of 0.8, 1.0, 1.2 and 1.3

The magnitude and signs of Markstein length indicates the effect of stretch on flame propagation. Positive Markstein length indicates that stretched flame speed decreases as stretch rate increases and the flame tend to restrain any disturbance at the flame front leading to flame stability [18]. In this case, the surface convex to the unburned area will be stretched in the opposite direction, and this will suppress flame speed, and the flame stabilizes. On the contrary, negative Markstein length indicates that flame speed increases proportionally with stretch rate, and flame surface will stretch in the same direction, inducing flame front instability in the process. Obviously from Figure 7, Markstein length for each equivalence ratio is positive with different magnitude as indicated by their relative slope. This difference will be discussed later.

Figure 8 shows the Markstein length variation with respect to equivalence ratio. Markstein length of each run is the average value of duplicate experiment. The plot of Markstein length against equivalence ratio illustrates how the Markstein length changes with fuel concentration. There is a noticeable difference between the trend especially compared to observation by Gu *et al.* and Rozenchan *et al.* [6, 7]. Apparently, in this study the determined Markstein length varies exponentially with equivalence ratio just as the case in study by [9]. This indicates the prevalence of stretch on flame speed at richer equivalence ratio and this corresponds to the exponential increase in Markstein length with equivalence ratio. This also implies that stable flames are expected in the richer region as can be observed in Figure 2. The basis for this observation is that the density ratio of the unburned to the burned gas increases proportionally to equivalence ratio in lean region followed by a decrease in flame thickness [20].

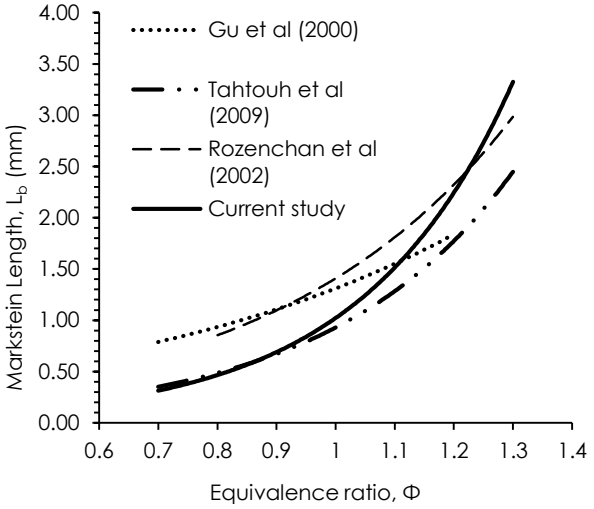

Figure 8 Comparison of Markstein length from literature and current study atequivalence ratio from 0.7 to 1.3

Figure 9 shows the comparison of burning rates of methane-air mixturewith respect to equivalence ratio between previous studies and current study. The burning rate variation with equivalence ratio shows a quadratic trend with a characteristics peak at equivalence ratio of 1.1. This is characteristics of combustion where highest burning rate is observed at equivalence ratio slightly larger than stoichiometric due to mixing of fuel and oxidizer.

As shown in Figure 9, at equivalence ratio of 1.3, the burning rate is higher in this study at 0.31 m/s compared to observations by Rozenchan *et al.* [7] and Egolfopoulus *et al.* [21] at 0.28 m/s, while Taylor [5] recorded the slowest burning rate at 0.21 m/s. This could be linked to the slightly higher initial temperature for this experiment at 302K. Marginal increase in unburned gas temperature may consequently increase the burning rate [22].

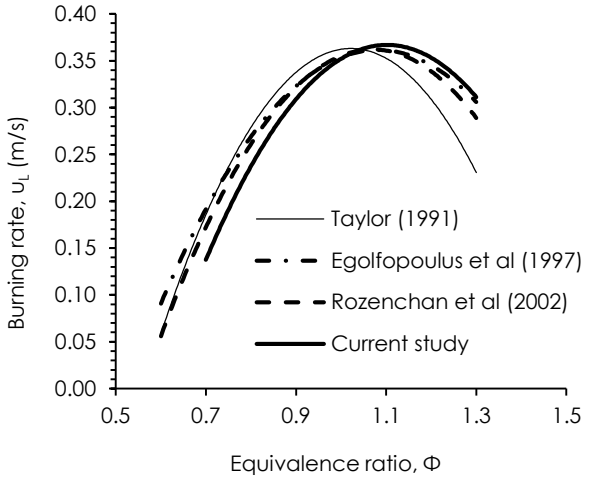

Figure 9 Comparison of methane-air mixture burning rate between present and previous works at equivalence ratio from 0.7 to 1.3

Different methodology and the quality of data obtained from each study could also lead to different results [9]. This could be observed by results from [21] that used the counterflow methodology to determine the burning rate of methane-air mixture while both [5 & 7] used recorded Schlieren images of spherically expanding flame. Different analysis of the same data could also yield different results as reported by [9] that used three different techniques namely the polynomial fitting, differentiation of raw radius, and resolution of Clavin's equation to link flame speed and stretch linearly.

4.0 CONCLUSION

In the present work, the combustion of methane has been studied by analyzing the spherical propagation flame of methane-air mixture in terms of flame development, flame speed, burning rate and Markstein length. Smooth and stable spherical flames were observed throughout flame development for all equivalence ratios. However, small fluctuations at later stage of flame development were observed suggesting the presence of acoustic disturbance. This fluctuation varies from 6.8% to 19.0% as equivalence ratio was increased from 0.7 to 1.3, suggesting the influence of equivalence ratio on acoustic disturbance.

The burning rate and Markstein length from this study shows a good agreement in comparison with the previous works. Apart from the experimental methodology, the quality of images obtained, image processing and the methods of data analysis could be considered as the source of uncertainties. Markstein length variation with equivalence ratio shares similarity with work by [9]. The largest variation in terms of burning rate could be observed in the case of experiment with equivalence ratio of 1.3. This probably caused by the difference in initial temperature of this particular experiment which is slightly higher at 302K.

Acknowledgement

The authors would like to thank Ministry of Higher Education of Malaysia and Universiti Teknologi Malaysia for supporting this research activity under the research grant scheme Q.J130000.2524.07H55 and R.J130000.7824.4F749.

References

[1] Bosschaart, K. J., de Goey, L. P. H. 2004. The Laminar Burning Velocity of Flames Propagating in Mixtures of Hydrocarbons and Air Measured with the Heat Flux Method. *Combust. Flame*. 136: 261-269.

[2] Konnov, A. A., Dyakov, I. V., De Ruyck, J. 2003. Measurement of Adiabatic Burning Velocity in Ethane–Oxygen–Nitrogen and in Ethane–Oxygen–Argon Mixtures. Exp. *Therm. Fluid Sci*. 27: 379-384.

[3] Chao, B. H., Egolfopoulos, F. N., Law, C. K. 1997. Structure and Propagation of Premixed Flame in Nozzle-Generated Counterflow, *Combust. Flame*. 109: 620–638.

[4] Jackson, G. S., Sai, R., Plaia, J. M., Boggs, C. M., Kiger, K. T. 2003. Influence of H_2on the Response of Lean Premixed CH4 Flames to High Strained Flows. *Combust. Flame*. 132: 503-511.

[5] Taylor, S. C. 1991. Burning Velocity and The Effect Of Flame Stretch. PhD Thesis. University of Leeds.

[6] Gu, X. J., Haq, M. Z., Lawes, M., Woolley, R. 2000. Laminar Burning Velocity and Markstein Lengths of Methane–Air Mixtures. *Combust. Flame*. 121: 41-58.

[7] Rozenchan, G., Zhu, D. L., Law, C. K., Tse, S. D. 2002. Outward Propagation, Burning Velocities, and Chemical Effects of Methane Flames up to 60 Atm. *Proceedings of the Combustion Institute*. 29: 1461-1469.

[8] Hassan, M. I., Aung, K. T., Faeth, G. M. 1998. Measured and Predicted Properties of Laminar Premixed Methane/Air Flames at Various Pressures. *Combust. Flame*. 115: 539-550.

[9] Tahtouh, T., Halter, F., Mounaim-Rousselle, C. 2009. Measurement of Laminar Burning Speeds and Markstein Lengths Using a Novel Methodology. *Combustion and Flame*. 156: 1735-1743.

[10] Gillespie, L., Lawes, M., Sheppard, C. G. W., and Woolley, R. 2000. Aspects of Laminar and Turbulent Burning Velocity Relevant to SI Engines. *Society of Automotive Engineers*. 2000-01-0192.

[11] Hinton, N., Stone, R. 2014. Laminar Burning Velocity Measurements of Methane and Carbon Dioxide Mixtures (Biogas) Over Wide Ranging Temperatures and Pressures. *Fuel*. 116: 743-750.

[12] Bradley, D., Hicks, R. A., Lawes, M., Sheppard, C. G. W., and Woolley, R. 1998. The Measurement of Laminar Burning Velocities and Markstein Numbers for Iso-octane–Air and Iso-octane–nHeptane–Air Mixtures at Elevated Temperatures and Pressures in an Explosion Bomb. *Combustion and Flame*. 115(1-2): 126-144.

[13] Turns, S. R. 2012. *An Introduction to Combustion: Concepts and Applications*. 3rd edition. New York: McGraw Hill.

[14] Bradley, D., Lung, K. K. 1987. Spark Ignition and the Early Stages of Turbulent Flame Propagation. *Combust. Flame*. 69: 71-93.

[15] Zhang, Z., Guan, D., Zheng, Y., and Li, G. 2015. Characterizing Premixed Laminar Flame–Acoustics Nonlinear Interaction.*Energy Conversion and Management*. 98: 331-339.

[16] Shalaby, H., Luo, K. H., Thévenin, D. 2014. Response of Curved Premixed Flames to Single-Frequency and Wideband Acoustic Waves. *Combustion and Flame*. 161: 2868-2877.
[17] Movileanu, C., Gosa, V., Razus, D. 2015. Propagation of Ethylene–Air Flames in Closed Cylindrical Vessels with Asymmetrical Ignition. *Process Safety and Environmental Protection*. 96: 167-176.
[18] Bradley, D., Gaskell, P., Gu, X. 1996. Burning Velocities, Markstein Lengths, and Flame Quenching for Spherical Methane–Air Flames: A Computational Study. *Combustion and Flame*. 104(1-2):176-98.
[19] Poinsot, T., Veynante, D. 2005. *Theoretical and Numerical Combustion*. 2nd edition. Philadelphia: R.T. Edwards.
[20] Miao, H., Liu, Y. 2014. Measuring the Laminar Burning Velocity and Markstein Length of Premixed Methane/Nitrogen/Air Mixtures with the Consideration of Nonlinear Stretch Effects. *Fuel*. 121: 208-215.
[21] Egolfopoulus, F. N., Cho, P., and Law, C. K. 1989. Laminar Flame Speeds of Methane-Air Mixtures under Reduced and Elevated Pressures. *Combustion and Flame*. 76 (3-4): 375-391.
[22] Bradley, D., Hundy, G. F. 1971. Burning Velocities of Methane-Air Mixtures Using Hot-Wire Anemometers in Closed-Vessel Explosions. *Symposium (International) on Combustion*. 13(1): 575-583.